national accelerator laboratory

TM-485
0428

Magnetic Field Distribution in Doubler Type Dipoles

S.C. Snowdon

April 2, 1974

Summary

A direct calculation is made of the two dimensional magnetic field from a conductor of wedge shaped cross section carrying a uniform current distribution. For sufficiently small conductors the wedge shape simulates the keystoned conductor used in doubler type magnets. Field distributions are presented for the dual test dipoles, the doubler dipole, and the muon beam line dipole. A similar calculation representing the contribution of the magnet ends to the longitudinally integrated fields is also given for the same magnets.

Magnetic Field of Single Conductor in Doubler Geometry

Using complex notation the dipole magnetic field ($H = H_x + iH_y$) for variable current density conductors and images is given by

$$H^* = -2i \iint J \left\{ \frac{1}{z-z_o-d} - \frac{1}{z+z_o+d} + \frac{1}{z-z_o^*-d} - \frac{1}{z+z_o^*+d} + \frac{1}{z-\frac{R_i^2}{z_o^*+d}} - \frac{1}{z+\frac{R_i^2}{z_o^*+d}} + \frac{1}{z-\frac{R_i^2}{z_o+d}} - \frac{1}{z+\frac{R_i^2}{z_o+d}} \right\} r_o dr_o d\theta_o \quad (1)$$

where $z_o = r_o e^{i\theta}$ and integration is required only over the conductor located in the first quadrant. See. Fig. 1 for geometrical details.

If J is either constant as in the two-dimensional case or a function only of θ_o as is convenient and reasonably realistic in the case of the end contributions which will be treated later, it is possible to integrate over the radial extent of the conductor. Individual integrals become

$$T_1(z) = \int_{R_1}^{R_2} \frac{r_o dr_o}{z-d-e^{i\theta_o}}$$

$$= e^{-2i\theta_o}\left[-(R_2-R_1)e^{i\theta_o} - (z-d)\ \ln\left(\frac{z-d-R_2e^{i\theta_o}}{z-d-R_1e^{i\theta_o}}\right)\right], \tag{2}$$

$$T_2(z) = \int_{R_1}^{R_2} \frac{r_o dr_o}{z+d+r_oe^{i\theta_o}}$$

$$= e^{-2i\theta_o}\left[(R_2-R_1)e^{i\theta_o} - (z+d)\ \ln\left(\frac{z+d+R_2e^{i\theta_o}}{z+d+R_1e^{i\theta_o}}\right)\right], \tag{3}$$

$$T_3(z) = \int_{R_1}^{R_2} \frac{r_o dr_o}{z-d-e^{i\theta_o}}$$

$$= e^{2i\theta_o}\left[-(R_2-R_1)e^{-i\theta_o} - (z-d)\ \ln\left(\frac{z-d-R_2e^{-i\theta_o}}{z-d-R_1e^{-i\theta_o}}\right)\right], \tag{4}$$

$$T_4(z) = \int_{R_1}^{R_2} \frac{r_o dr_o}{z+d+r_oe^{-i\theta_o}}$$

$$= e^{2i\theta_o}\left[(R_2-R_1)e^{-i\theta_o} - (z+d)\ \ln\left(\frac{z+d+R_2e^{-i\theta_o}}{z+d+R_1e^{-i\theta_o}}\right)\right], \tag{5}$$

$$S_1(z) = \int_{R_1}^{R_2} \frac{d+r_o e^{-i\theta_o}}{z(d+r_o e^{-i\theta_o})-R_i^2} \cdot r_o dr_o$$

$$= \frac{1}{2} \cdot \frac{R_2^2-R_1^2}{z} + (R_2-R_1) \cdot \frac{R_i^2}{z^2} e^{i\theta_o}$$

$$+ \frac{e^{2i\theta_o}}{z^3} \cdot R_i^2(R_i^2-zd) \ln\left[\frac{z(d+R_2 e^{-i\theta_o})-R_i^2}{z(d+R_1 e^{-i\theta_o})-R_i^2}\right], \tag{6}$$

$$S_2(z) = {}_{R_1}^{R_2} \frac{d+r_o e^{-i\theta_o}}{z(d+r_o e^{-i\theta_o})+R_i^2} \cdot r_o dr_o$$

$$= \frac{1}{2} \cdot \frac{R_2^2-R_1^2}{z} - (R_2-R_1) \cdot \frac{R_i^2}{z^2} e^{i\theta_o}$$

$$+ \frac{e^{2i\theta_o}}{z^3} \cdot R_i^2(R_i^2+zd) \ln\left[\frac{z(d+R_2 e^{-i\theta_o})+R_i^2}{z(d+R_1 e^{-i\theta_o})+R_i^2}\right], \tag{7}$$

$$S_3(z) = \int_{R_1}^{R_2} \frac{d+r_o e^{i\theta_o}}{z(d+r_o e^{i\theta_o})-R_i^2} \cdot r_o dr_o$$

$$= \frac{1}{2} \cdot \frac{R_2^2-R_1^2}{z} + (R_2-R_1) \cdot \frac{R_i^2}{z^2} e^{-i\theta_o}$$

$$+ \frac{e^{-2i\theta_o}}{z^3} \cdot R_i^2(R_i^2-zd) \ln\left[\frac{z(d+R_2 e^{i\theta_o})-R_i^2}{z(d+R_1 e^{i\theta_o})-R_i^2}\right], \tag{8}$$

$$S_4(z) = \int_{R_1}^{R_2} \frac{d+r_o e^{i\theta_o}}{z(d+r_o e^{i\theta_o})+R_i^2} \cdot r_o dr_o$$

$$= \frac{1}{2} \cdot \frac{R_2^2-R_1^2}{z} - (R_2-R_1) \cdot \frac{R_i^2}{z^2} e^{-i\theta_o}$$

$$+ \frac{e^{-2i\theta_o}}{z^3} \cdot R_i^2(R_i^2+zd) \ln \left[\frac{z(d+R_2 e^{i\theta_o})+R_i^2}{z(d+R_1 e^{i\theta_o})+R_i^2} \right] \tag{9}$$

The resultant field from one conductor suitably located in each quadrant to give a dipole field is

$$H^*(z) = -2i \int_{\theta_1}^{\theta_2} J(\theta_o)\, R(z,\theta_o) d\theta_o \quad , \tag{10}$$

where

$$R(z,\theta_o) = T_1-T_2+T_3-T_4+S_1-S_2+S_3-S_4 \ . \tag{11}$$

Since z occurs in the denominator of the S-expressions one must evaluate these carefully for z = o. Thus

$$R(0,\theta_o) = -4(R_2-R_1) \cos\theta_o + 2de^{-2i\theta_o} \ln\left(\frac{d+R_2 e^{i\theta_o}}{d+R_1 e^{i\theta_o}}\right)$$

$$+ 2de^{2i\theta_o} \ln\left(\frac{d+R_2 e^{-i\theta_o}}{d+R_1 e^{-i\theta_o}}\right)$$

$$- 2\,\frac{d(R_2^2-R_1^2)}{R_i^2} - \frac{4}{3}\,\frac{R_2^3-R_1^3}{R_i^2} \cos\theta_o \ . \tag{12}$$

For the case of constant current density it would be possible to carry out the θ_o-integration analytically. However, this is not done since a numerical integration technique must be developed for the variable case. Thus Eq. (10) is the final result for a single

conductor in the first quadrant. Summation of similar results for other conductors located in the first quadrant gives the general result.

Longitudinally Integrated Magnetic Field

If a current distribution is localized in space and w is an axial coordinate orthogonal to the transverse coordinates x and y, Lambertson and others[1] have shown that by integrating the field equations along the w-axis from $-\infty$ to $+\infty$

$$\frac{\partial}{\partial x}\int H_y \, dw - \frac{\partial}{\partial y}\int H_x \, dw = 4\pi \int J_w \, dw \, , \tag{13}$$

and

$$\frac{\partial}{\partial x}\int H_x \, dw + \frac{\partial}{\partial y}\int H_y \, dw = 0. \tag{14}$$

These equations may be put into the complex notation for ease of calculation by defining

$$G_x = \int_{-\infty}^{\infty} H_x \, dw \, , \tag{15}$$

$$G_y = \int_{-\infty}^{\infty} H_y \, dw \, , \tag{16}$$

and

$$K = \int_{-\infty}^{\infty} J_w \, dw \, . \tag{17}$$

Then, Eqs. (13-14) become[2] using $G = G_x + iG_y$.

$$\frac{\partial G^*}{\partial z^*} = -2\pi i K \tag{18}$$

or, in integral form for the dipole symmetry considered here (z is outside the current)

$$G^* = -2i\iint K\left\{\frac{1}{z-z_o-d} - \frac{1}{z+z_o+d} + \frac{1}{z-z_o^*-d} - \frac{1}{z+z_o^*+d}\right.$$

$$\left. + \frac{1}{z-\frac{R_i^2}{z_o^*+d}} - \frac{1}{z+\frac{R_i^2}{z_o^*+d}} + \frac{1}{z-\frac{R_i^2}{z_o+d}} - \frac{1}{z+\frac{R_i^2}{z_o+d}}\right\} r_o dr_o d\theta_o \quad (19)$$

By comparing this with Eq. (5) one sees that the longitudinally integrated fields are distributed in the transverse coordinates as in a two-dimensional problem. The integrated fields replace the actual field and the integrated current density replaces the normal current density.

Magnet End Development

The conductor placement at the ends of the magnet is considered to be developed[3] from a flat curve in which connection between the two parallel sides is made by means of a semicircular arc. The details of the developed surface are presented in Fig. 2a. After the layer of conductors has been unwrapped, the parallel sides are described by

$$a = \frac{1}{2}(R_1+R_2)(\frac{\pi}{2} - \theta_o), \quad (20)$$

$$s = \frac{1}{2}(R_1+R_2)(\frac{\pi}{2} - \theta) , \quad (21)$$

$$b = \frac{1}{2}(R_1+R_2)(\frac{\pi}{2} - \theta_1). \quad (22)$$

By assumption the unwrapped lager has a round end (Fig. 2b). Hence the current density in the axial direction is

$$J_w = J_o \cos\phi = J_o \frac{t}{\sqrt{w^2+t^2}} \quad . \tag{23}$$

Integrating this axially gives

$$K = \int J_w dw = J_o t \int_\alpha^\beta \frac{dw}{\sqrt{w^2+t^2}} \quad , \tag{24}$$

where

$$\alpha = \left\{ \begin{matrix} \sqrt{g^2-t^2} & \text{for} & t < g \\ 0 & \text{for} & t > g \end{matrix} \right\} \quad , \tag{25}$$

and

$$\beta = \sqrt{h^2-t^2} \quad . \tag{26}$$

Hence the contribution of a single end to the integrated current is

$$K(\theta) = J_o t \left\{ \begin{matrix} \ln\left(\dfrac{\sqrt{h^2-t^2}+h}{\sqrt{g^2-t^2}+g} \right) \\ \ln\left(\dfrac{\sqrt{h^2-t^2}+h}{t} \right) \end{matrix} \right\} \quad . \tag{27}$$

Note further, that any transverse straight section in the s-direction may be added without affecting Eq. (27) other than through the choice of origin of s.

Application

Many factors are involved in arriving at a suitable disposition of conductors. In general one desires the integrated fields to be as uniform as possible with a tolerance level in $\Delta B/B$ definitely below 0.1% in the useful aperture. The total amount of superconductor used to achieve the desired central field must be kept to a minimum. This is accomplished in these designs by using two different sizes of superconductor, the large cross section being used in the highest field regions and the smaller cross section in the lower field regions. The criterion for the wire choice in each region is that some fraction of the critical current density must not be exceeded. Another general consideration in line with the critical current requirement stems from noting that the magnetic field at the conductors in the end region tends to be higher than the central field. This can be modified by choosing different axial lengths for each layer, by terminating the iron shielding short of the ends, and by "dogboning" the turns with the highest curvature.

There is no general method of optimizing the quality of the integrated field that incorporates all of these considerations. We chose to proceed as follows. Technical Services[4], using a multipole expansion equivalent of the two-dimensional calculation reported here carried out the initial exploration of conductor locations in the body of the magnet and produced high field quality choices consistent with allowing fluid passages and a return bus conductor. These conductor locations were then inserted into LINDA, a magnetostatic iterative program, to determine the dividing line between the use of the two conductor types.

Technical Services again produced a high quality field utilizing the restriction introduced by LINDA. Practical magnet ends were then developed by Technical Services and modified after LINDA runs of the end configurations suggested a reasonable iron termination that would give no field rise over the central field. The net configuration was examined for field quality of the integrated fields. The difference between this quality and the previous high quality two dimensional adjustments were then used by Technical Services to obtain a field variation that could just be compensated by the application of magnet ends. This final configuration was tested by obtaining the integrated fields. All the results presented here follow from the above mentioned procedure.

Results

Computer output records all the necessary input and giving median plane variation of the coil contribution, image or iron contribution, and resulting field. Two cases are considered for the doubler, Mark I and Mark II. For each case the distribution of the median plane field within the magnet body (Calculational Mode = 0) and the distribution of the median plane integrated field (Calculated Mode = 1) is given. The results for Mark II are definitely superior to those of Mark I and it is expected that further fine adjustments will provide even higher quality fields.

Similar results are given for the Mark I version of the large aperture muon beam line dipole.

References

1. Robert B. Meuser, "End Effect in Superconducting Beam Transport Magnets", IEEE Trans. Nucl. Sci. NS-18, 677 (1971). Integral theorem is attributed to G.R. Lambertson.
2. W.W. Lee and S.C. Snowdon, "Design of Dipole Magnet with Circular Iron Shield", IEEE Trans. Nucl. Sci. NS-20, 726 (1973).
3. M.A. Green, "The Elimination of High Multipoles in the Two Dimensional and Integrated Fields of Conductor-Dominated Dipole and Quadrupole Magnets with Iron Sheets", Lawrence Berkeley Laboratory UCID-3493 (Jan. 15, 1971).
4. Work carried out by G. Biallas.

Figure 1. Legend

0 = Center

F = Right Hand Origin

F' = Left Hand Origin

z_1 = Image Position of z_o

R_1 = Inner Radius of Wedge Conductor ($F-R_1$)

R_2 = Outer Radius of Wedge Conductor ($F-R_2$)

R_i = Inner Radius of Iron ($0-P$)

d = Offset ($F'-0$ or $0-F$)

$$H^* = 2iI\left(\frac{1}{z-z_o} + \frac{1}{z-z_1}\right)$$

$$z_o = \left\{\begin{matrix} d+r_o e^{i\theta_o} & \text{Right Hand Wedge} \\ -d+r_o e^{i\theta_o} & \text{Left Hand Wedge} \end{matrix}\right\}$$

$$z_1 = R_i^2/z_o^*$$

$$I = J\, r_o dr_o d\theta_o$$

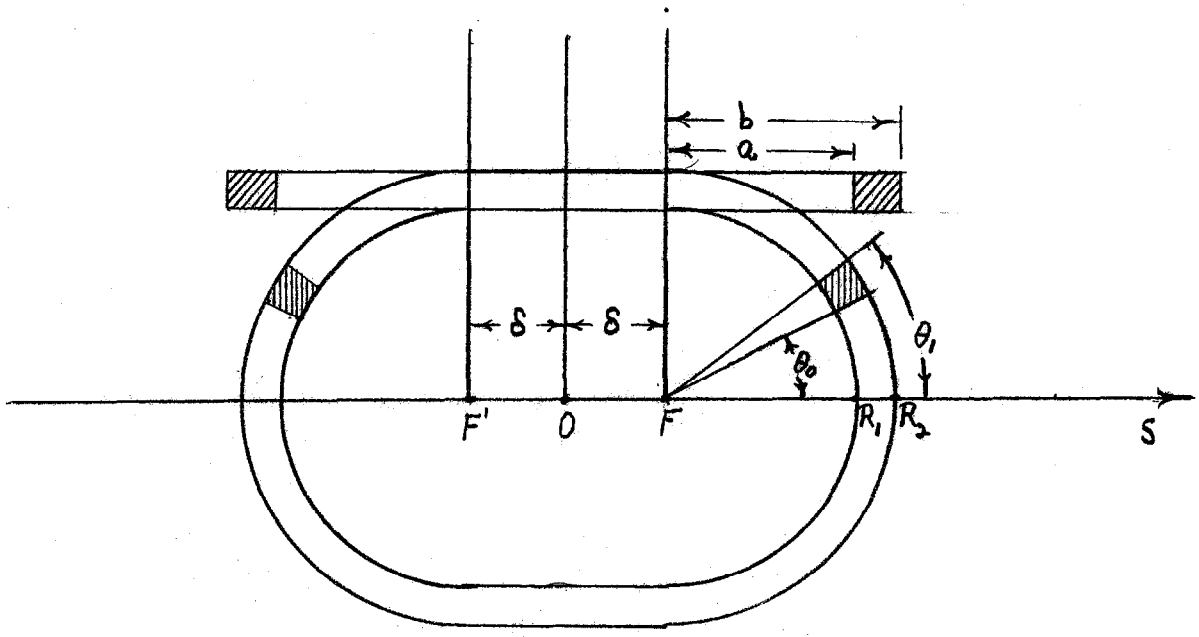

Figure 2a. Unwrapping of Conductor (See Legend)

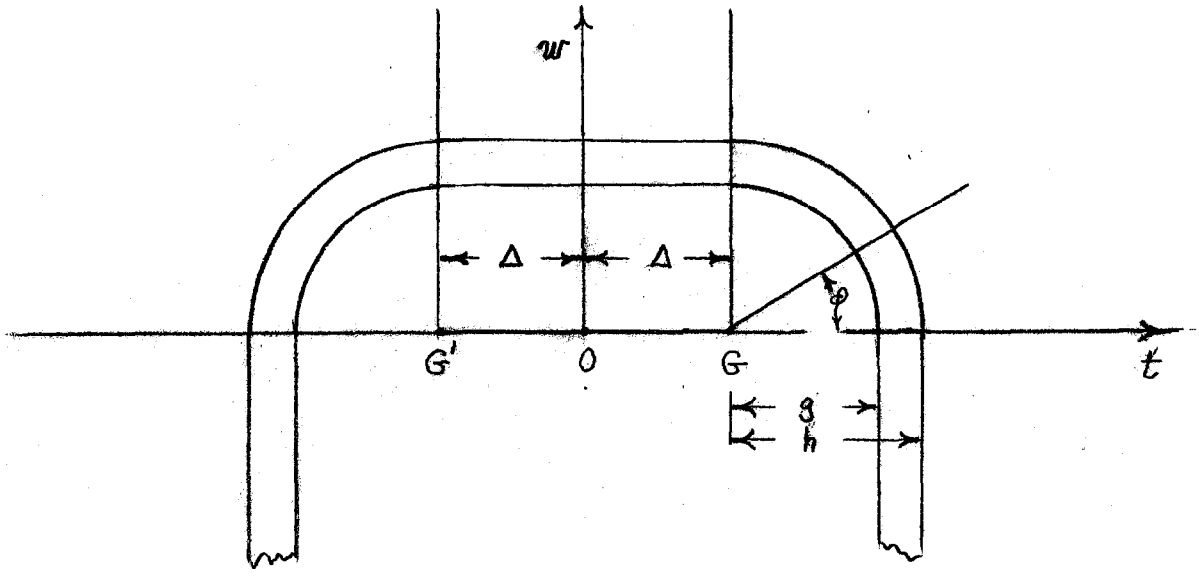

Figure 2b. Plan View of Unwrapped Conductor (See Legend)

DIRECT INTEGRATION OF SHELL MODEL DOUBLER MAGNET Mark I

CALCULATIONAL MODE	=	0	NUMBER OF LAYERS	=	8		
CONDUCTOR CURRENT(A)	=	2815.0000	REFERENCE RADIUS(IN)	=	1.0000	INNER IRON RADIUS(IN)	= 3.0000
SIMPSONS RULE INTERVAL(DEG)	=	1.0000	HORIZONTAL INCREMENT(IN)	=	.1000	HORIZONTAL OFFSET(IN)	= .3750
FLAT BEND CENTER(IN)	=	0.0000	INSULATION THICKNESS(IN)	=	.0015		

LAYER	TURNS	CURDEN (KA/IN/IN)	THETAS (DEG)	THETAF (DEG)	SPACER (IN)	RINNER (IN)	ROUTER (IN)	LENGTH (IN)
1	18.0000	268.0200	0.0000	76.7019	0.0000	.8750	1.0326	1.0000
2	22.0000	408.2161	0.0000	51.5719	0.0000	1.0954	1.2516	1.0000
3	16.0000	407.4277	0.0000	33.2774	0.0000	1.2530	1.4085	1.0000
4	4.0000	267.1165	53.0960	67.1163	0.0000	1.0954	1.2516	1.0000
5	2.0000	268.1132	82.4773	90.9972	0.0000	.8750	1.0326	1.0000
6	3.0000	267.1543	68.9841	79.4979	0.0000	1.0954	1.2516	1.0000
7	1.0000	268.0644	91.1576	95.4032	0.0000	.8790	1.0365	1.0000
8	3.0000	407.4216	41.5394	47.7790	0.0000	1.2530	1.4085	1.0000

X(IN)	BT(KG-IN)	BA(KG-IN)	BS(KG-IN)	BN
0.00000	-44.42070	-35.32926	-8.59144	1.00000
.10000	-44.41655	-35.32419	-8.59236	.99991
.20000	-44.40436	-35.30924	-8.59511	.99963
.30000	-44.38493	-35.28522	-8.59971	.99919
.40000	-44.35962	-35.25348	-8.60614	.99862
.50000	-44.33018	-35.21576	-8.61442	.99796
.60000	-44.29849	-35.17395	-8.62455	.99725
.70000	-44.26519	-35.12966	-8.63654	.99652
.80000	-44.23428	-35.08390	-8.65039	.99580
.90000	-44.20264	-35.03652	-8.66612	.99509
1.00000	-44.16931	-35.08558	-8.68373	.99434
1.10000	-44.12059	-35.42635	-8.70324	.99345
1.20000	-44.07445	-35.34979	-8.72466	.99221
1.30000	-37.98374	-29.24074	-8.74800	.85520

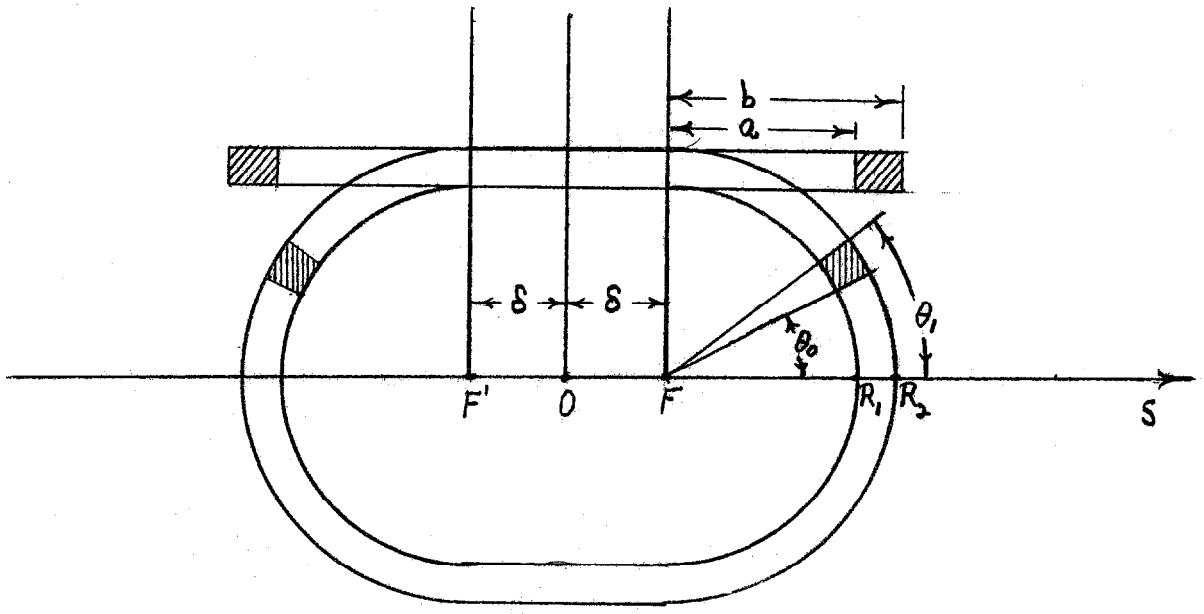

Figure 2a. Unwrapping of Conductor (See Legend)

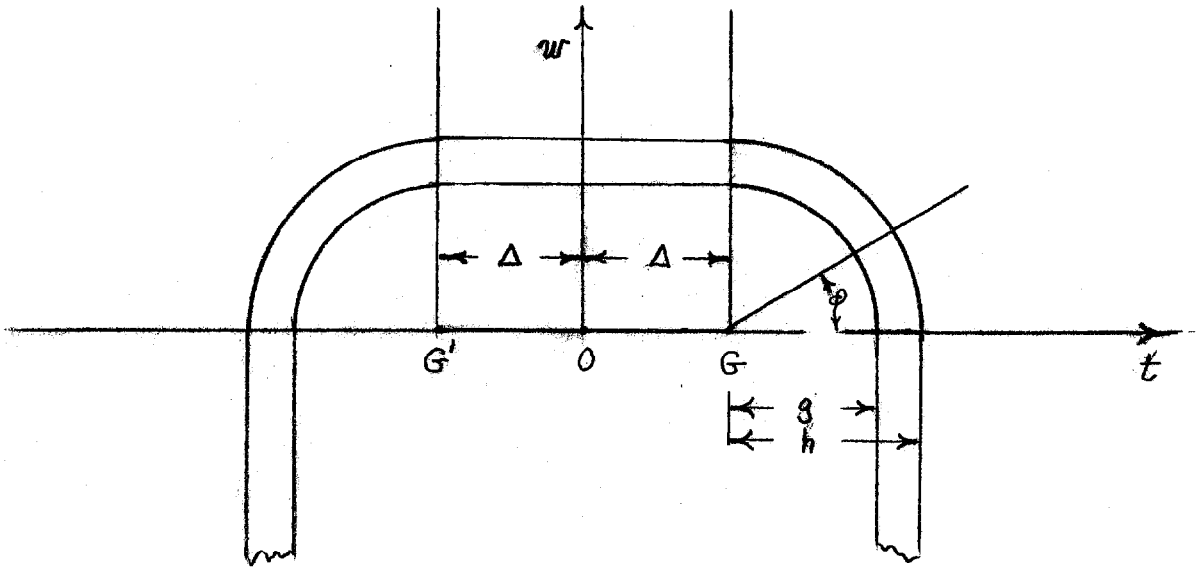

Figure 2b. Plan View of Unwrapped Conductor (See Legend)

DIRECT INTEGRATION OF SHELL MODEL DOUBLER MAGNET Mark 1

CALCULATIONAL MODE	= 0	NUMBER OF LAYERS	= 8				
CONDUCTOR CURRENT(A)	= 2815.0000	REFERENCE RADIUS(IN)	= 1.0000	INNER IRON RADIUS(IN)	= 3.0000		
SIMPSONS RULE INTERVAL(DEG)	= 1.0000	HORIZONTAL INCREMENT(IN)	= .1000	HORIZONTAL OFFSET(IN)	= .3750		
FLAT BEND CENTER(IN)	= 0.0000	INSULATION THICKNESS(IN)	= .0015				

LAYER	TURNS	CURDEN (KA/IN/IN)	THETAS (DEG)	THETAF (DEG)	SPACER (IN)	RINNER (IN)	ROUTER (IN)	LENGTH (IN)
1	13.0000	268.0200	0.0000	76.7019	0.0000	.8750	1.0326	1.0000
2	22.0000	408.2161	0.0000	51.5719	0.0000	1.0954	1.2516	1.0000
3	16.0000	407.4277	0.0000	33.2774	0.0000	1.2530	1.4085	1.0000
4	4.0000	267.1165	53.0960	67.1163	0.0000	1.0954	1.2516	1.0000
5	2.0000	268.1132	82.4773	90.9972	0.0000	.8750	1.0326	1.0000
6	3.0000	267.1543	68.9941	79.4979	0.0000	1.0954	1.2516	1.0000
7	1.0000	268.0644	91.1576	95.4032	0.0000	.8790	1.0365	1.0000
8	3.0000	407.4216	41.5394	47.7790	0.0000	1.2530	1.4085	1.0000

X(IN)	BT(KG-IN)	BA(KG-IN)	BS(KG-IN)	BN
0.00000	-44.42070	-35.32926	-8.59144	1.00000
.10000	-44.41655	-35.32419	-8.59236	.99991
.20000	-44.40436	-35.30924	-8.59511	.99963
.30000	-44.38493	-35.28522	-8.59971	.99919
.40000	-44.35962	-35.25348	-8.60614	.99862
.50000	-44.33018	-35.21576	-8.61442	.99796
.60000	-44.29849	-35.17395	-8.62455	.99725
.70000	-44.26619	-35.12966	-8.63654	.99652
.80000	-44.23428	-35.08390	-8.65039	.99580
.90000	-44.20264	-35.03652	-8.66612	.99509
1.00000	-44.16931	-35.48558	-8.68373	.99434
1.10000	-44.12059	-35.42635	-8.70324	.99345
1.20000	-44.07445	-35.34079	-8.72466	.99221
1.30000	-37.98874	-29.24074	-8.74800	.85520

DIRECT INTEGRATION OF SHELL MODEL DOUBLER MAGNET Mark II

CALCULATIONAL MODE	=	0	NUMBER OF LAYERS	=	8		
CONDUCTOR CURRENT(A)	=	2815.0000	REFERENCE RADIUS(IN)	=	1.0000	INNER IRON RADIUS(IN)	= 3.0625
SIMPSONS RULE INTERVAL(DEG)	=	1.0000	HORIZONTAL INCREMENT(IN)	=	.1000	HORIZONTAL OFFSET(IN)	= .3750
FLAT BEND CENTER(IN)	=	0.0000	INSULATION THICKNESS(IN)	=	.0015		

LAYER	TURNS	CURDEN (KA/IN/IN)	THETAS (DEG)	THETAF (DEG)	SPACER (IN)	RINNER (IN)	ROUTER (IN)	LENGTH (IN)
1	16.0000	267.4469	.1662	68.4856	0.0000	.8750	1.0326	1.0000
2	3.0000	267.4161	77.3493	90.1606	0.0000	.8750	1.0326	1.0000
3	1.0000	267.5583	94.5380	98.7493	0.0000	.8892	1.0466	1.0000
4	22.0000	407.5915	.1318	51.7954	0.0000	1.0950	1.2512	1.0000
5	4.0000	266.7569	53.0960	67.1392	0.0000	1.0950	1.2512	1.0000
6	3.0000	266.7939	75.6304	86.1614	0.0000	1.0950	1.2512	1.0000
7	16.0000	406.9258	.1146	33.3805	0.0000	1.2550	1.4105	1.0000
8	5.0000	407.0132	39.3049	49.5984	0.0000	1.2550	1.4105	1.0000

X(IN)	BT(KG-IN)	BA(KG-IN)	BS(KG-IN)	BN
0.00000	-44.37571	-35.99964	-8.37607	1.00000
.10000	-44.37435	-35.99747	-8.37688	.99997
.20000	-44.37089	-35.99160	-8.37929	.99989
.30000	-44.36704	-35.98373	-8.38331	.99980
.40000	-44.36477	-35.97583	-8.38895	.99975
.50000	-44.36515	-35.96896	-8.39619	.99976
.60000	-44.36704	-35.96199	-8.40505	.99980
.70000	-44.36624	-35.95071	-8.41553	.99979
.80000	-44.35551	-35.92789	-8.42762	.99954
.90000	-44.32518	-35.88385	-8.44133	.99886
1.00000	-44.26335	-35.80667	-8.45667	.99747
1.10000	-44.15287	-35.67923	-8.47364	.99498
1.20000	-43.94330	-35.45106	-8.49224	.99026
1.30000	-37.80176	-29.28929	-8.51247	.85186

DIRECT INTEGRATION OF SHELL MODEL DOUBLER MAGNET **Mark II**

CALCULATIONAL MODE	= 1	NUMBER OF LAYERS	= 8		
CONDUCTOR CURRENT(A)	= 2815.0000	REFERENCE RADIUS(IN)	= 1.0000	INNER IRON RADIUS(IN)	= 3.0625
SIMPSONS RULE INTERVAL(DEG)	= 1.0000	HORIZONTAL INCREMENT(IN)	= .1000	HORIZONTAL OFFSET(IN)	= .3750
FLAT BEND CENTER(IN)	= 0.0000	INSULATION THICKNESS(IN)	= .0015		

LAYER	TURNS	CURDEN (KA/IN/IN)	THETAS (DEG)	THETAF (DEG)	SPACER (IN)	RINNER (IN)	ROUTER (IN)	LENGTH (IN)
1	16.0000	267.4469	.1662	68.4856	0.0000	.8750	1.0326	239.5460
2	3.0000	267.4161	77.3493	90.1606	0.0000	.8750	1.0326	239.5460
3	1.0000	267.5583	94.5380	98.7493	0.0000	.8892	1.0466	239.5460
4	22.0000	407.5915	.1318	51.7954	0.0000	1.0950	1.2512	241.1230
5	4.0000	266.7569	53.0960	67.1392	0.0000	1.0950	1.2512	241.1230
6	3.0000	266.7939	75.6304	86.1614	0.0000	1.0950	1.2512	241.1230
7	16.0000	406.9258	.1146	33.3805	0.0000	1.2550	1.4105	240.8060
8	5.0000	407.0132	39.3049	49.6984	0.0000	1.2550	1.4105	240.8060

X(IN)	BT(KG-IN)	BA(KG-IN)	BS(KG-IN)	BN
0.00000	-10798.72067	-8759.60174	-2039.11894	1.00000
.10000	-10798.26402	-8758.95109	-2039.31293	.99996
.20000	-10797.04798	-8757.15291	-2039.89497	.99985
.30000	-10795.47259	-8754.60740	-2040.86519	.99970
.40000	-10794.00004	-8751.77619	-2042.22384	.99956
.50000	-10792.86361	-8748.89235	-2043.97125	.99946
.60000	-10791.75391	-8745.64607	-2046.10784	.99935
.70000	-10780.61133	-8740.97724	-2048.63409	.99916
.80000	-10734.61675	-8733.06618	-2051.55057	.99869
.90000	-10774.32625	-8719.46837	-2054.85789	.99774
1.00000	-10755.69237	-8697.13569	-2058.55668	.99602
1.10000	-10724.26145	-8661.61382	-2062.64763	.99310
1.20000	-10667.14596	-8600.01455	-2067.13141	.98782
1.30000	-9181.96758	-7109.95890	-2072.00868	.85028

DIRECT INTEGRATION OF SHELL MODEL MUON MAGNET MARK I

CALCULATIONAL MODE	= 1	NUMBER OF LAYERS	= 5				
CONDUCTOR CURRENT(A)	= 2380.0000	REFERENCE RADIUS(IN)	= 2.2500	INNER IRON RADIUS(IN)	= 5.7500		
SIMPSONS RULE INTERVAL(DEG)	= 1.0000	HORIZONTAL INCREMENT(IN)	= .1000	HORIZONTAL OFFSET(IN)	= 1.0000		
FLAT BEND CENTER(IN)	= 0.0000	INSULATION THICKNESS(IN)	= .0015				

LAYER	TURNS	CURDEN (KA/IN/IN)	THETAS (DEG)	THETAF (DEG)	SPACER (IN)	RINNER (IN)	ROUTER (IN)	LENGTH (IN)
1	48.0000	224.5244	.0630	87.0895	0.0000	2.2500	2.4031	120.0000
2	1.0000	224.6759	93.4150	95.2199	0.0000	2.2590	2.4121	120.0000
3	50.0000	342.5520	.0573	55.6858	0.0000	2.4650	2.6179	122.9980
4	16.0000	224.3136	55.6858	82.2997	0.0000	2.4650	2.6179	124.4060
5	39.0000	342.5256	.0516	39.9237	0.0000	2.6220	2.7747	122.9980

X(IN)	BT(KG-IN)	BA(KG-IN)	BG(KG-IN)	BN
0.00000	-5078.21699	-3787.62242	-1290.59458	1.00000
.10000	-5078.27443	-3787.63130	-1290.64313	1.00001
.20000	-5078.44350	-3787.65474	-1290.78876	1.00004
.30000	-5078.71484	-3787.68331	-1291.03153	1.00010
.40000	-5079.07350	-3787.70203	-1291.37148	1.00017
.50000	-5079.50831	-3787.69133	-1291.80868	1.00025
.60000	-5079.97167	-3787.62843	-1292.34324	1.00035
.70000	-5080.46402	-3787.48974	-1292.97528	1.00044
.80000	-5080.95239	-3787.24747	-1293.70492	1.00054
.90000	-5081.41335	-3786.88102	-1294.53232	1.00063
1.00000	-5081.82586	-3786.36818	-1295.45768	1.00071
1.10000	-5082.17207	-3785.69090	-1296.48118	1.00078
1.20000	-5082.43752	-3784.83448	-1297.60304	1.00083
1.30000	-5082.61068	-3783.78719	-1298.82350	1.00087
1.40000	-5082.68179	-3782.53899	-1300.14281	1.00088
1.50000	-5082.64083	-3781.07959	-1301.56125	1.00087
1.60000	-5082.47477	-3779.39567	-1303.07910	1.00084
1.70000	-5082.16410	-3777.46742	-1304.69668	1.00078
1.80000	-5081.67471	-3775.26441	-1306.41430	1.00068
1.90000	-5080.97334	-3772.74105	-1308.23229	1.00054
2.00000	-5079.98269	-3769.83168	-1310.15101	1.00035
2.10000	-5078.61650	-3766.44569	-1312.17081	1.00008
2.20000	-5076.75466	-3762.46260	-1314.29206	.99971
2.30000	-5074.24267	-3757.72753	-1316.51514	.99922
2.40000	-5070.88729	-3752.04687	-1318.94042	.99856
2.50000	-5066.45222	-3745.18392	-1321.26830	.99768
2.60000	-5060.65269	-3736.95353	-1323.79915	.99654
2.70000	-5053.14626	-3726.71287	-1326.43339	.99506
2.80000	-5043.51326	-3714.34189	-1329.17137	.99317
2.90000	-5031.20918	-3699.19570	-1332.01348	.99074
3.00000	-5015.43274	-3680.47266	-1334.96009	.98764
3.10000	-4994.66195	-3656.65032	-1338.01154	.98355
3.20000	-4963.51933	-3622.35117	-1341.16815	.97741
3.30000	-4317.58157	-2973.15129	-1344.43028	.85022